Part 2: Turbomole Calculations

1. Structural properties of the ground state

The molecular structure of oligo[2,7-(fluorene)-co-*alt*-2,5-pyridine]$_n$, $(FPy)_n$, containing also the bond numbering used in this work is depicted in Figure 20. The ground state torsional potential energy curve around the interring bond no. 7 of the fluorene-pyridine monomer, (FPy) as obtained from B3LYP/SVP calculations is shown in Figure 21. The potential energy curve for the ground state shows two minima. One on the cis side (taking the Py nitrogen and the H side chain of F group as reference) and the other one at the trans side. Both minima are energetically very close. The cis minimum has been fully optimized and a torsional angle of 14.4° was found. The energy barrier to planarity is very small (0.03 kcal/mol). The cis-trans barrier is 5.56 kcal/mol which is higher than that obtained for the biphenyl barrier (1.80 kcal mol) (Beenken *et al.*, 2005). This higher barrier affected in a consequence of the bulky fluorene and pyridine units as compared with phenylene units.

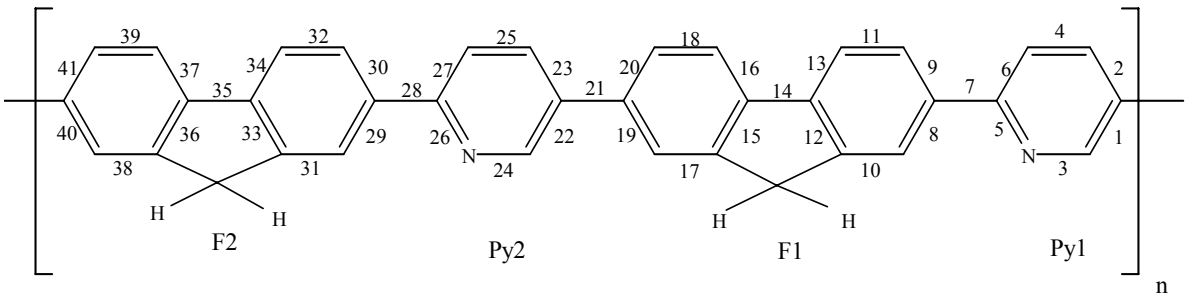

Figure 20 Molecular structure and numbering scheme of oligo[2,7-(fluorene)-co-*alt*-2,5-pyridine]$_n$, $(FPy)_n$.

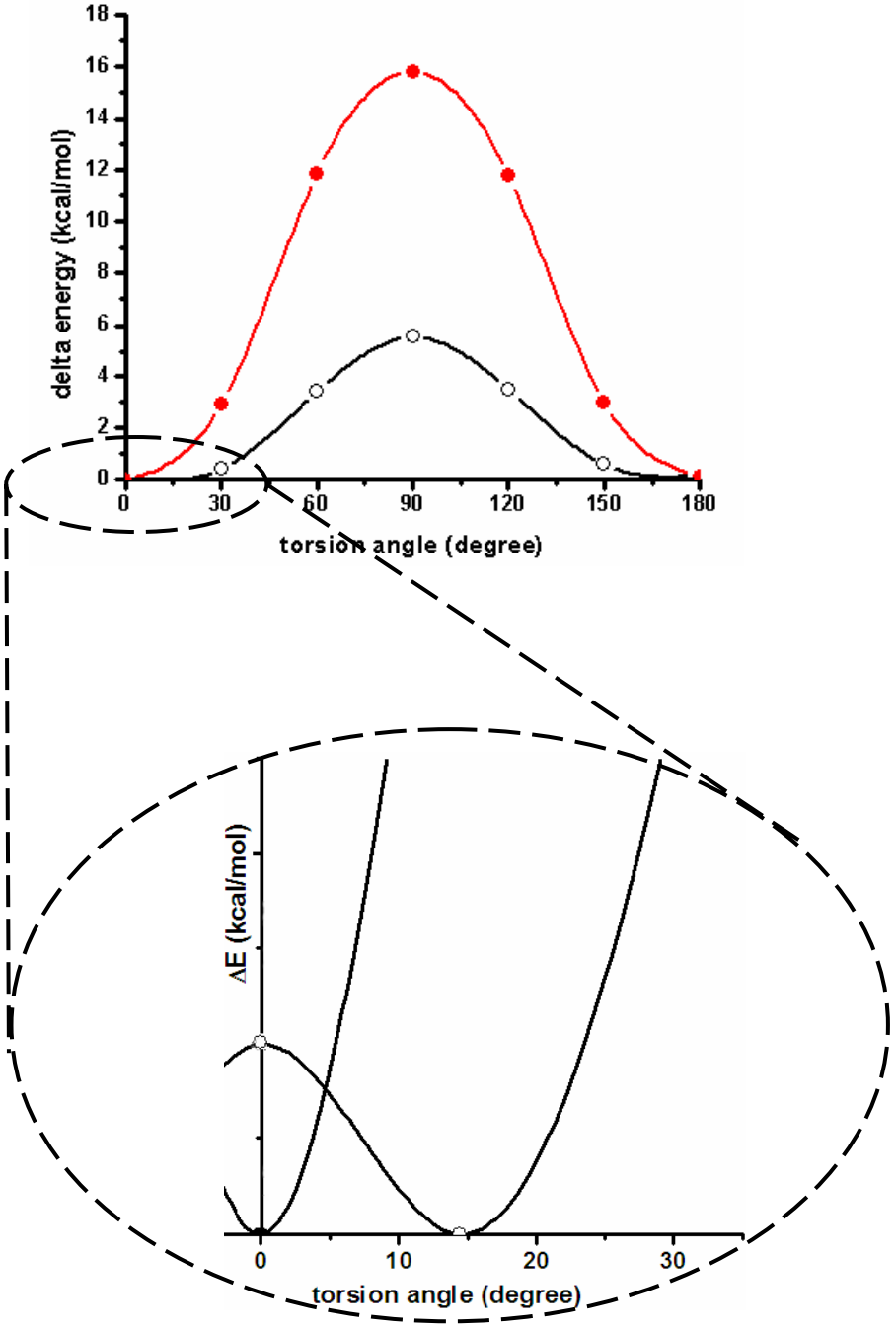

Figure 21 Torsional potential energy curves around bond 7 (see Figure 20) for the ground state of the FPy monomer as obtained from B3LYP/SVP (black circle) calculations and the lowest excited state as computed using the TDDFT/B3LYP/SVP approach (red circle). Energies are given with respect to the energy minimum of the respective state with torsional angles of 14.4° for the ground state and 0.1° for the excited state.

The ground state potential curves of FPy dimer as calculated from B3LYP/SVP calculations are illustrated in Figure 22. Each potential curve for the ground state revealed two minima. The energy barriers as obtained from F1-Py1, Py2-F1 and F2-Py2 are 4.78, 2.37 and 5.03 kcal/mol, respectively. The optimized torsional angles of F1-Py1 (bond number 7), Py2-F1 (bond number 21) and F2-Py2 (bond number 28) are -15.9, 37.1 and -8.6^{o}, respectively. The results implied that the Py2-F1 torsional angle (bond number 21) is higher than that obtained from F1-Py1 and F2-Py2. The Py2-F1 is the middle torsional angle of the dimer molecule which was fixed by fluorene, pyridine on the left and also fluorene and pyridine on the right.

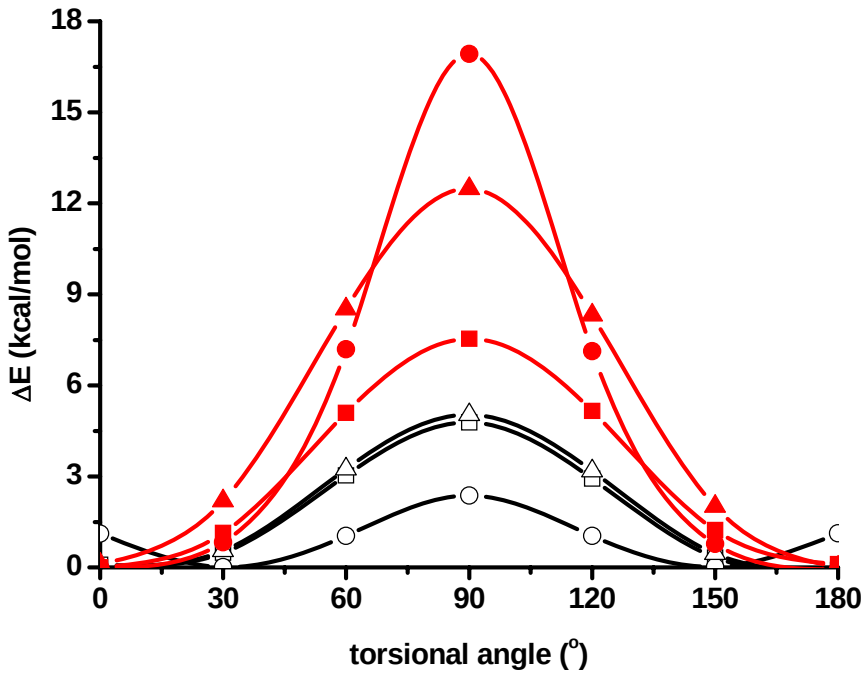

Figure 22 Torsional potential energy curves around bonds 7 (black squares), 21 (black circles) and 28 (black triangles) (see Figure 20) for the ground state of the FPy should be dimer as obtained from B3LYP/SVP calculations and for the lowest excited state using the TDDFT/B3LYP/SVP approach (red squares, red circles and red triangles, respectively).

Optimized bond lengths obtained with the B3LYP/SVP and TD-B3LYP/SVP methods are displayed in Figure 23. Selected interring distances and the corresponding interring torsional angles are summarized in Table 23. Most interesting from the point of view of interring torsional modes are the bond distances connecting the fluorene and pyridine rings and the related torsions between pyridine and fluorene unitsPy-F and F-Py (Table 23) along the oligomer chain. From Table 23, it is found that the interring bond distances do not display appreciable variation with the oligomer size in the series of $(FPy)_n$. However, there is a remarkable change in the torsional angles Py1-F1, Py2-F2, Py3-F3, Py4-F4 and F1-Py2, F2-Py3 and F3-Py4F-Py and Py-F. Whereas the former angle tends towards planarization when increasing the chain length the latter angle is thereby practically unaffected and keeps a value of about 35°. The interring torsional angles Py1-F1, Py2-F2, Py3-F3, Py4-F4 tend to be closer to planarity even though the corresponding interring distances are large as compared with the interring distances of F1-Py2, F2-Py3 and F3-Py4. In this latter case the interring torsional angles remain to be large with values around 35°. These results suggested that there exists a weak hydrogen bonded interaction between the hydrogen atom of fluorene and the nitrogen atom of the pyridine unit. For the Py1-F1, Py2-F2, Py3-F3, Py4-F4F-Py units no such possibility for hydrogen bonding is available. Additionally, no steric hindrance between N and the neighboring fluorene exists in case of Py-F.

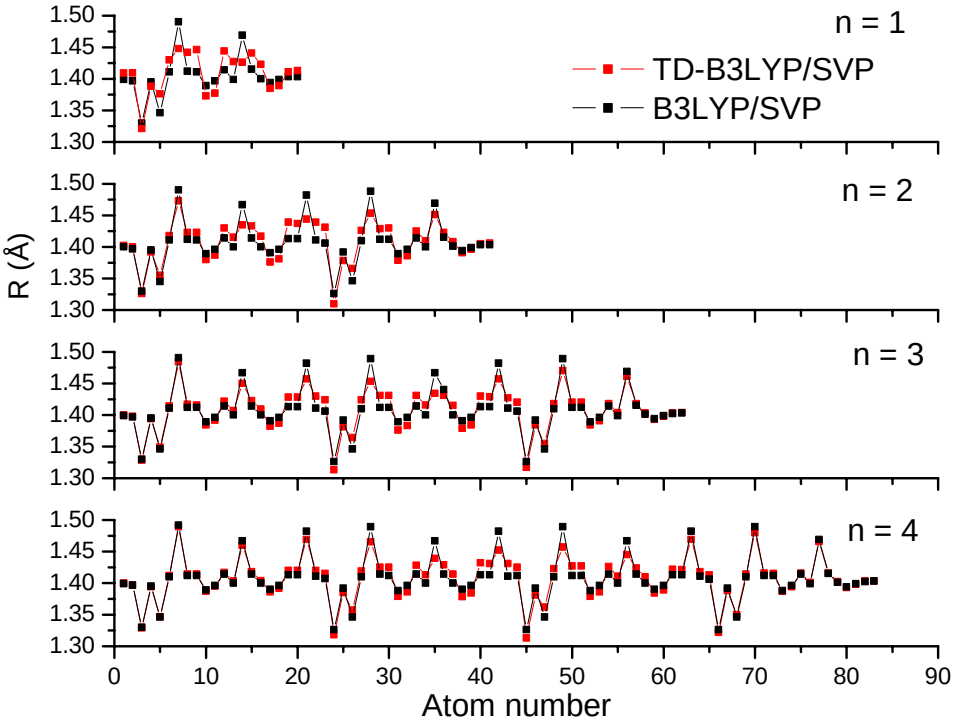

Figure 23 Optimized bond lengths (Å) of $(FPy)_n$ in the ground state (S_0) and the lowest excited state (S_1), obtained from B3LYP/SVP (black circle) and TD-B3LYP/SVP (red square) calculations.

Table 23 Optimized interring distance, d (Å) and torsion angle, ϕ (deg) of $(FPy)_n$ (n=1-4) in the ground state (S_0) and the lowest excited state (S_1), obtained from B3LYP/SVP and TD-B3LYP/SVP calculations.

	monomer		dimer		trimer		tetramer	
	S_0	S_1	S_0	S_1	S_0	S_1	S_0	S_1
	B3LYP/SVP	TD-B3LYP/ SVP	B3LYP/SVP	TD-B3LYP/ SVP	B3LYP/SVP	TD-B3LYP/ SVP	B3LYP/SVP	TD-B3LYP/ SVP
d_7	1.490	1.448	1.490	1.473	1.491	1.484	1.492	1.489
d_{14}	1.469	1.426	1.467	1.435	1.467	1.450	1.467	1.460
d_{21}			1.482	1.444	1.482	1.457	1.482	1.469
d_{28}			1.488	1.453	1.489	1.453	1.489	1.465
d_{35}			1.469	1.451	1.467	1.434	1.467	1.439
d_{42}					1.482	1.457	1.482	1.452
d_{49}					1.489	1.470	1.489	1.457
d_{56}					1.469	1.461	1.467	1.445
d_{63}							1.482	1.469
d_{70}							1.489	1.480
d_{77}							1.469	1.466
ϕ_{Py1-F1}	-14.4	-0.1	-15.9	-0.5	9.7	0.5	-1.5	-1.0
ϕ_{F1-Py2}			37.1	9.4	-36.3	-16.8	34.5	26.5
ϕ_{Py2-F2}			-8.6	0.1	-9.7	-0.2	-6.2	-0.2
ϕ_{F2-Py3}					35.9	19.2	35.3	16.5
ϕ_{Py3-F3}					7.0	2.0	0.6	0.6
ϕ_{F3-Py4}							35.8	26.9
ϕ_{Py4-F4}							-1.4	1.8

Py denotes the pyridine ring and F the fluorene ring.

2. Vertical excitation energies

The TDDFT/B3LYP/SVP and TDDFT/B3LYP/SVP+sp methods were used on the basis of the ground state optimized structures to compute vertical electronic excitation energies of all oligomers investigated in this work. The first 5 singlet electronic transitions and oscillator strengths of FPy oligomers are listed in Table 24. Agreement between TDDFT/SVP and SVP+sp results is within 0.1 eV.

Table 24 Calculated and experimental excitation energies and oscillator strengths of fluorene-pyridine oligomers.

		TD-B3LYP/SVP		TD-B3LYP/SVP+sp	
	state	excitation energy, (eV)	oscillator strength	excitation energy, (eV)	oscillator strength
n=1	S_1	3.96	0.852	3.88	0.831
	S_2	4.36	0.019	4.26	0.032
	S_3	4.47	0.006	4.45	0.009
	S_4	4.59	0.011	4.50	0.007
	S_5	4.61	0.009	4.55	0.009
n=2	S_1	3.31	1.994	3.27	1.967
	S_2	3.78	0.055	3.74	0.053
	S_3	3.93	0.082	3.85	0.082
	S_4	4.14	0.014	4.06	0.015
	S_5	4.18	0.025	4.11	0.006
n=3	S_1	3.09	2.922	3.05	2.882
	S_2	3.48	0.239	3.44	0.286
	S_3	3.52	0.178	3.47	0.123
	S_4	3.78	0.042	3.74	0.028
	S_5	3.81	0.482	3.76	0.476
n=4	S_1	2.99	3.640	2.95	3.584
	S_2	3.26	0.739	3.22	0.744
	S_3	3.36	0.138	3.32	0.124
	S_4	3.53	0.443	3.48	0.423
	S_5	3.56	0.005	3.53	0.044
n=∞	S_1	2.66		2.64	
Expt. [a]	S_1	3.20(thin film) 3.26(THF solution)			

[a] = Aubert *et al.* 2004

From the analysis of the wave function given in Table 25 it is clearly indicated that the transition to the S_1 state is characterized predominantly by the promotion of an electron from the highest occupied molecular orbital (HOMO) to the lowest unoccupied molecular orbital (LUMO) whereas the HOMO-1→ LUMO transition is the main character of the $S_0 \rightarrow S_2$ transition (Table 25). For all oligomers the $S_1 \leftarrow S_0$ electronic transition revealed the largest oscillator strength. However, it is found that with increasing chain length the other transitions increase considerably in intensity.

Table 25 Dominant orbital contributions for the first lowest excitation energies of FPy oligomers using B3LYP/SVP geometries.

Oligomers	state	MO/character (Dominant contributions)
		TD-B3LYP/SVP
n=1	$S_0 \rightarrow S_1$	HOMO→LUMO (97%)
	$S_0 \rightarrow S_2$	HOMO→LUMO+1 (54%)
	$S_0 \rightarrow S_3$	HOMO-3→LUMO (70%)
	$S_0 \rightarrow S_4$	HOMO→LUMO+2 (42%)
	$S_0 \rightarrow S_5$	HOMO-1→LUMO (57%)
n=2	$S_0 \rightarrow S_1$	HOMO→LUMO (98%)
	$S_0 \rightarrow S_2$	HOMO-1→LUMO (68%)
	$S_0 \rightarrow S_3$	HOMO→LUMO+1 (67%)
	$S_0 \rightarrow S_4$	HOMO-5→LUMO (34%)
	$S_0 \rightarrow S_5$	HOMO→LUMO+3 (38%)
n=3	$S_0 \rightarrow S_1$	HOMO→LUMO (92%)
	$S_0 \rightarrow S_2$	HOMO-1→LUMO (93%)
	$S_0 \rightarrow S_3$	HOMO→LUMO+1 (92%)
	$S_0 \rightarrow S_4$	HOMO-2→LUMO (69%)
	$S_0 \rightarrow S_5$	HOMO-1→LUMO+1 (86%)
n=4	$S_0 \rightarrow S_1$	HOMO→LUMO (83%)
	$S_0 \rightarrow S_2$	HOMO-1→LUMO (60%)
	$S_0 \rightarrow S_3$	HOMO→LUMO+1 (56%)
	$S_0 \rightarrow S_4$	HOMO-1→LUMO+1 (86%)
	$S_0 \rightarrow S_5$	HOMO-2→LUMO (79%)

In Figure 24, the S_1 excitation energies are plotted against the inverse number of repeat units. A good linear relationship is found. The extrapolated excitation energies to infinite chain length at TDDFT/B3LYP/SVP and TDDFT/B3LYP/SVP+sp levels

are 2.66 and 2.64 eV, respectively. The extrapolated vertical excitation energy is somewhat lower than the experimental values (3.20 eV in film and 3.26 eV in THF solution, Aubert *et al.*, 2004). Previous experience with TDDFT/B3LYP calculations on methylene-bridged oligofluorenes showed that this approach underestimated the extrapolated excitation energies (Lukeš *et al.*, 2005). Another reason might be that the effective conjugation length is smaller due to defects in the polymer chains.

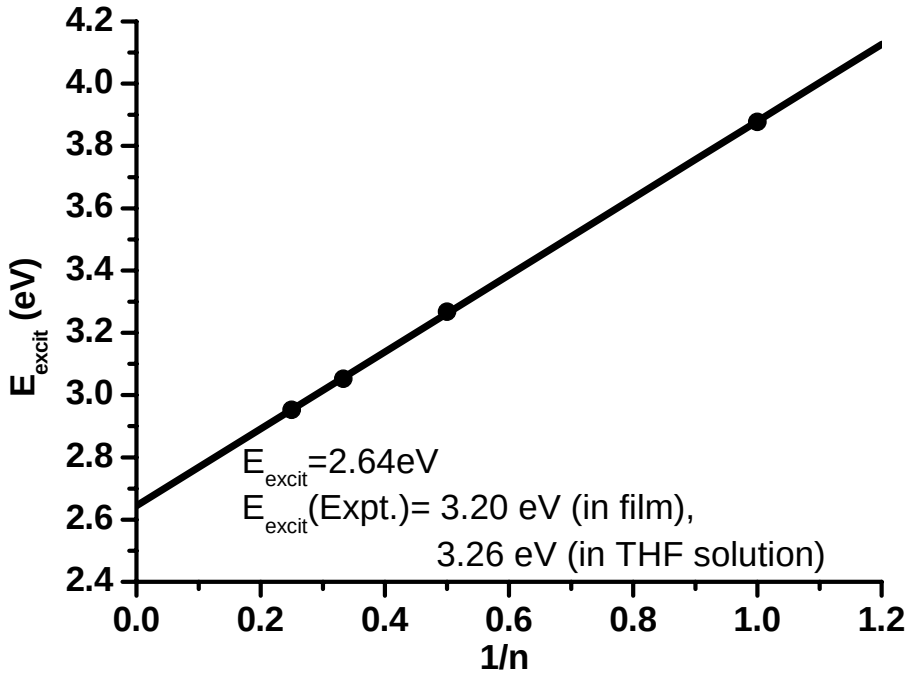

Figure 24 The lowest excitation energies (E_{excit}) computed by the TD-DFT/SVP+sp method as a function of reciprocal chain length n of the oligomers $(FPy)_n$.

3. Structural properties of the lowest excited singlet state

The geometrical parameters optimized for the S_1 state of different oligomers are displayed in Figure 3. As can be seen, the bond distances along the long axis of the molecule, bond numbers 2, 5, 7, 9, 12, 14, 16, 19 in the monomer (Figure 20), are significantly shortened in comparison to the ground state. For example, the interring bond distance No. 7 is reduced from 1.490 Å in the ground state to 1.448 Å in the first excited state. In contrast, the other bond distances are significantly elongated. This

clearly demonstrates that the structure of lowest excited state acquire quinoidic character. In agreement with this finding, the FPy oligomers obtain a more planarized conformation. The torsional angle around the interring bond 7 in the monomer is reduced from 14.1° in the ground state to 0.1° in S_1. For the torsional angles in the larger oligomers see Table 1. The Py-F torsional angles are again closer to planarity than the F-Py angle due to hydrogen bonding and steric hindrance as explained in structural properties of the ground state section for the ground state. Nevertheless, the F-Py angles are reduced also in agreement with the shortening of corresponding interring distances.

It is instructive to analyze the HOMO and LUMO describing the lowest singlet excitation. These orbitals are shown in Figure 25 for the monomer and the tetramer. The HOMO and LUMO are delocalized practically along the entire π-conjugated backbone with the HOMO more concentrated on the side with the fluorene termination and the LUMO more localized toward the other end. Thus, on excitation into the LUMO a charge transfer toward the pyridine end will occur. The HOMO is characterized by intraring bonding. On the other hand, there is significant interring bonding between the bridge atoms in the LUMO. These features explain nicely the shortenings of the interring distances and the planarization in the excited state.

The potential energy curve for the lowest excited state (S_1) for the FPy monomer, computed at the TD-DFT/SVP level is displayed in Figure 21. There are two well defined minima at 0° and 180° which reveal a completely planar structure in the excited state. An energy barrier of 15.8 kcal/mol is located between the two minima. This barrier is significantly larger than the one found for the ground state (5.5 kcal/mol). This increase is in line with the decrease of the aforementioned interring distance and the concomitant reduction of the torsional angles.

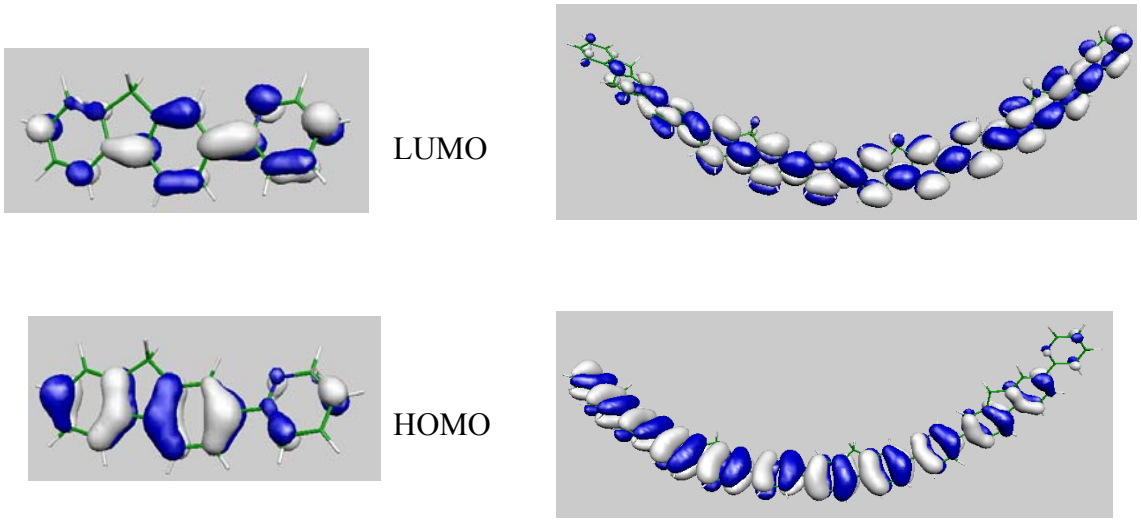

(a) (FPy) (b) $(FPy)_4$

Figure 25 Plots of HOMO and LUMO of (FPy) and $(FPy)_4$ obtained by the TD-B3LYP/SVP+sp approach.

The excited state potential energy curves of the fluorene-pyridine dimer as obtained by the TD-DFT/SVP approach are shown in Figure 22. The excited state potential energy curves display two minima. The energy barrier as calculated for F1-Py1, Py2-F1 and F2-Py2 are 7.53, 16.93 and 12.48 kcal/mol, respectively. The torsional angles between two adjacent units are reduced in the excited state as compared to the ground state. It was found that the torsional angles between F1-Py1, Py2-F2 and F2-Py2 units are reduced from -15.9° to -0.5°, 37.1° to 9.4° and -8.6° to 0.1°, respectively. Consequently, the excited state structure of the dimer comes closer to planarity.

4. Fluorescence energies and Lifetimes

Fluorescence energies computed with the TDDFT/B3LYP/SVP and TDDFT/B3LYP/SVP+sp methods using S_1 optimized geometries (TDDFT/SVP) are collected in Table 26. In Figure 26 the linear relationship between the fluorescence energies on the reciprocal chain lengths is demonstrated. The extrapolated

fluorescence energies obtained from the TDDFT/B3LYP/SVP and TDDFT/B3LYP/SVP+sp methods are 2.41 and 2.16 eV, respectively. The basis set dependence of the fluorescence energies is somewhat larger than the one found for vertical excitation energies (see above). The fluorescence energies decrease with the extension of oligomers chain whereas the oscillator strengths increase. The fluorescence energies presented in Table 4 are lower than that of experimental data (Liu, S.P. *et al.*, 2005).

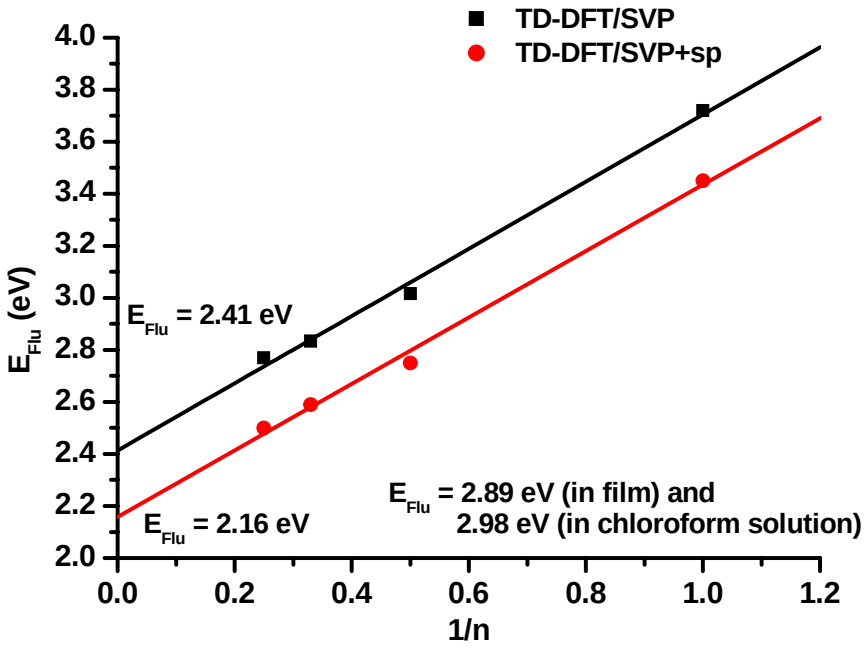

Figure 26 The dependence of fluorescence energies on the reciprocal chain length of $(FPy)_n$ as obtained from TD-DFT/SVP (solid square) and TD-DFT /SVP+sp (solid circle) calculations.

Table 26 Calculated fluorescence energies (oscillator strength in parentheses) and radiative lifetimes of FPy oligomers as obtained from TDDFT/B3LYP/SVP and TDDFT/B3LYP/SVP+sp calculations. Geometries were optimized at B3LYP/SVP level.

	TD-B3LYP/SVP		TD-B3LYP/SVP+sp	
	Fluorescence energy (eV)	Lifetime (ns)	Fluorescence energy (eV)	Lifetime (ns)
n=1	3.72 (0.996)	0.84	3.45 (0.984)	0.88
n=2	3.02 (2.335)	0.54	2.75 (2.291)	0.66
n=3	2.83 (3.202)	0.45	2.58 (3.149)	0.55
n=4	2.77 (3.786)	0.40	2.50 (3.752)	0.49
n=∞	2.41	0.25	2.16	0.38
expt.[a]	2.89 eV (in film) 2.98 eV (in chloroform)			

a = Liu, S.P. *et al.* (2005)

Radiative lifetimes were calculated on the basis of fluorescence energy and oscillator strengths according to the formula (in au) (Brandsen *et al.,* 1983)

$$\tau = \frac{c^3}{2\left(E_{\mathrm{Flu}}\right)^2 f} \qquad (1)$$

where c is the velocity of light, E_{Flu} is the fluorescence transition energy, and f is oscillator strength. Extension of the conjugated backbone leads to a decrease of lifetimes. Lifetimes extrapolated to n$\rightarrow \infty$ from B3LYP/SVP and B3LYP/SVP+sp data are 0.25 and 0.38 ns, respectively. The difference between the two basis sets is only 0.13 ns.